The Astrophysical Journal, 584:278–283, 2003 February 10

EXOTIC LENSING CORRECTIONS TO THE MICROLENSING OPTICAL DEPTH

J.-F. Glicenstein
DAPNIA-SPP, CE-Saclay, F-91191 Gif-sur-Yvette, France
Received 2002 July 5; accepted 2002 October 11

ABSTRACT

Microlensing surveys derive the microlensing optical depth toward various directions such as the Galactic center from the distribution of observed Einstein radius crossing times. I show that the formula that is being used is invalid for "exotic" lensing events. The corrected formula is derived. The "parallax" effect (Earth motion) requires no correction. Corrections for the finite sizes of sources and wide binary lenses are small (typically less than 1%), except for blended events. Corrections for intermediate-type binaries such as MACHO LMC-9 can be substantial.

Subject headings: dark matter — gravitational lensing

1. INTRODUCTION

Microlensing surveys (Paczyński 1996) such as EROS, MACHO, or the Optical Gravitational Lensing Experiment (OGLE) have been very successful at finding microlensing candidates. The MACHO collaboration (Alcock et al. 2000a) found 13–17 events in their 5.7 yr data sample toward the Large Magellanic Cloud (LMC). The EROS collaboration found four events toward the same direction in their 3 yr data (Lasserre et al. 2000; Lasserre 2000) and one event in the 2 yr Small Magellanic Cloud sample (Palanque-Delabrouille et al. 1998). Hundreds of microlensing events were found by either MACHO (Alcock et al. 2000c) or OGLE (Udalski et al. 1994) toward the Galactic center. EROS (Derue et al. 2001; Afonso 2001) also found tens of microlensing events toward the Galactic disk and the Galactic center.

The microlensing optical depth τ is given by

$$\tau = \int_o^{D_s} dD_d \, \pi r_{\rm E}^2 \rho_d(D_d) \, , \tag{1}$$

where D_d and D_s are the deflector and the source distance, $\rho_d(D_d)$ is the number density of deflectors of mass M_d, and $r_{\rm E}$, the Einstein radius, is given by

$$r_{\rm E} = \sqrt{\frac{4GM_d}{c^2}\frac{D_d(D_s - D_d)}{D_s}} \, . \tag{2}$$

The microlensing optical depth can be calculated toward any direction with a Galactic model. An interesting property of the optical depth is that it is independent of the deflector mass function. Since the deflector mass function is not known precisely (it is totally unknown in the case of halo microlensing), the comparison between predicted and measured optical depths is not very sensitive to systematics. The experimental determination of the optical depth is described in § 3.

The optical depth for microlensing toward the LMC measured by the MACHO collaboration is $\tau_{\rm LMC}^{\rm MACHO} = 1.2^{+0.4}_{-0.3} \times 10^{-7}$, a factor of 4 too small to explain the Galactic rotation curve. On the other hand, interpreting the observed optical depth in terms of lensing by known stellar populations in the Galactic disk or in the LMC seems difficult, since the expected contribution is much smaller [$\tau_{\rm stellar} = (0.24\text{–}0.36) \times 10^{-7}$]. The optical depth toward Baade's window measured by MACHO with red giants is $\tau = (2.0 \pm 0.4) \times 10^{-6}$ (Popowski et al. 2001). This seems somewhat (∼30%) too large compared to the predictions of models (Evans & Belokurov 2002). Previous measurements by MACHO (Alcock et al. 2000c) and OGLE (Udalski et al. 1994) were even larger by a factor of 1.5–2.

Systematic effects have been suspected as the reason for the excess optical depth toward the LMC and the Galactic center. The main suspect is the "blending"[1] of source stars, sometimes associated with binary lensing effects (see, e.g., Di Stefano 2000). The purpose of this paper is to investigate the role of "exotic" microlensing events in the calculation of the optical depth.

About 10% of the detected microlensing events are exotic events. They cannot be explained by the simplest point lens–point source (PLPS) model of lensing. Examples of exotic lenses are binary lenses or sources ("xallarap" events), "parallax" events (distortion due to the Earth's motion around the Sun), and events in which the disk of the source is differentially magnified (because of the finite size of the source). Since only 10% of the events are exotic, one naively expects a correction to the optical depth of at most 10% from exotic lensing. However, as is shown in § 4.3, the effect of exotic lensing is much stronger for blended events. Because of this, exotic events have a potentially large effect on the blending correction of the optical depth.

In §§ 2 and 3 I derive the expressions for the rate (eq. [14b]) and the contribution to the optical depth (eq. [21]) of exotic microlensing events.

2. THE MICROLENSING RATE

The Einstein radius crossing time $t_{\rm E}$ is the only physical information that can be obtained from most microlensing events. Once corrected for the experimental efficiency $\epsilon(t_{\rm E})$, the $t_{\rm E}$ distribution (or histogram) is an estimator $d\hat{\Gamma}/dt_{\rm E}$ of the differential microlensing rate $d\Gamma/dt_{\rm E}$:

$$\frac{d\hat{\Gamma}}{dt_{\rm E}} = \frac{1}{\epsilon(t_{\rm E})}\left(\frac{1}{N_{\rm src}T_{\rm obs}}\frac{dN_{\rm micr}}{dt_{\rm E}}\right) , \tag{3}$$

where $N_{\rm src}$, $T_{\rm obs}$, and $N_{\rm micr}$ are the number of sources, the

[1] The objects monitored by microlensing surveys are blends of many stars whose seeing disks are overlapping. Any of these stars can be lensed. Optical depth estimates include in general a blending correction.

total observing time, and the number of observed microlenses. A lensing event occurs whenever the magnification A of a microlensing event exceeds a threshold $A_{\rm thr}$ (in general, $A_{\rm thr} = 1.34$). For a given source, the locus of lens positions for which $A > A_{\rm thr}$ is called the "microlensing tube" (Griest 1991). It is easy to show that the number of lenses dN at distance D_d entering the microlensing tube and crossing an area $dl\, dD_d$ per unit time is

$$d\Gamma = \frac{d^2N}{dt} = \rho_d v_t\, dl\, dD_d\, \cos\theta f(v_t) v_t\, dv_t\, d\theta\ , \tag{4}$$

where $\boldsymbol{v}_t$ is the transverse velocity of the lens, $f(v_t)$ is the distribution of $v_t = ||\boldsymbol{v}_t||$, θ is the angle of $\boldsymbol{v}_t$ with respect to the normal to the tube section, and dl is the elementary length of the slice of the tube. The quantity v_t is related to $t_{\rm E}$ and $r_{\rm E}$ by

$$t_{\rm E} = \frac{r_{\rm E}}{v_t}\ , \tag{5}$$

and $d\Gamma$ is the number of lenses crossing inward through an area $dl\, dD_d$ of the microlensing tube per second. Hence, this is not the microlensing event rate, since a lens may enter the microlensing tube several times. However, the difference between these two rates is ignored until § 3.

The transverse velocity $\boldsymbol{v}_t$ is the sum of two components: the microlensing tube transverse drift velocity $\boldsymbol{v}_d$ and the velocity dispersion $\boldsymbol{v}_{\rm dis}$:

$$\boldsymbol{v}_t = \boldsymbol{v}_d + \boldsymbol{v}_{\rm dis}\ . \tag{6}$$

I assume hereafter that the velocity dispersion is distributed according to

$$\tilde{f}(\boldsymbol{v}_{\rm dis}) = \frac{1}{2\pi\sigma_x\sigma_y}\exp\left[-\left(\frac{v^2_{{\rm dis}(x)}}{2\sigma_x^2} + \frac{v^2_{{\rm dis}(y)}}{2\sigma_y^2}\right)\right]\ , \tag{7}$$

where x and y are the eigendirections of the velocity dispersion tensor. The quantity $\tilde{f}$ is normalized by

$$\int \tilde{f}\, dv_{{\rm dis}(x)}\, dv_{{\rm dis}(y)} = 1\ . \tag{8}$$

The orientation of the microlensing tube is arbitrary relative to the eigendirections of the velocity tensor. The transverse velocity distribution has to be averaged over all the orientations of the microlensing tube.

If the velocity dispersion tensor is isotropic with $\sigma_x = \sigma_y = \sigma$, the v_t distribution is given by

$$f(v_t) = \frac{1}{2\pi\sigma^2}\exp\left\{-\frac{1}{2\sigma^2}\left[v_t^2 + v_d^2 - 2v_t v_d\cos(\gamma + \Psi - \beta)\right]\right\}\ , \tag{9}$$

where the angles γ, Ψ, and β are defined in Figure 1. Averaging over $\alpha = \beta - \delta$ at fixed γ, Ψ, and δ gives

$$\begin{aligned}\bar{f}(v_t) &= \frac{1}{2\pi}\int_0^{2\pi} d\alpha f(v_t)\\ &= \frac{1}{2\pi\sigma^2}\exp\left\{-\left[\frac{1}{2\sigma^2}\left(v_t^2 + v_d^2\right)\right]\right\} I_0\left(\frac{2v_t v_d}{\sigma^2}\right)\ ,\end{aligned} \tag{10}$$

where I_0 is a modified Bessel function.

The general expression of $\bar{f}$ is cumbersome and is derived in the Appendix. It depends only on the kinematic variable v_d and is independent of the geometry of the microlensing tube.

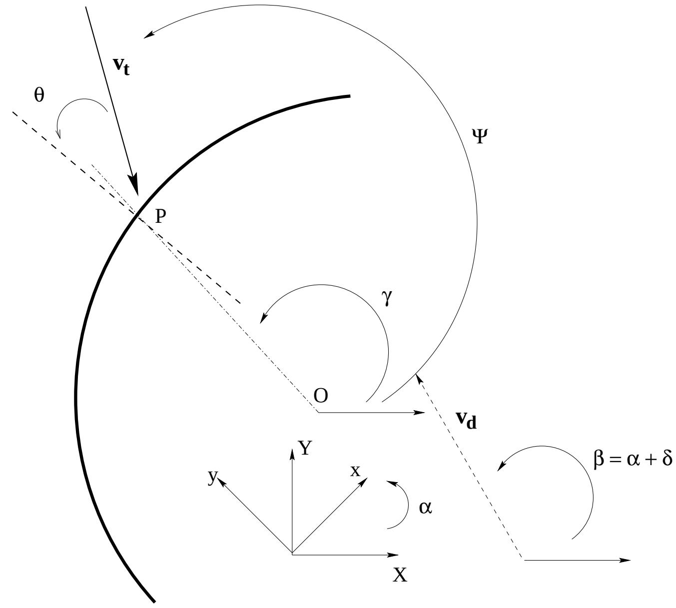

FIG. 1.—Section of the microlensing tube (*thick line*) perpendicular to the line of sight. The point O and the (X, Y)-axes are arbitrary. The point P is on the microlensing tube. The velocity tensor at P has principal axes (x, y). The normal to the slice of the microlensing tube is shown by the dashed line and is oriented outward. The angle between the X-axis and the x-axis is α. The drift velocity of the tube projected onto a plane perpendicular to the line of sight $\boldsymbol{v}_d$ makes an angle β with the X-axis.

Changing variables from v_t to $t_{\rm E}$ and integrating over θ gives

$$d\Gamma = 2\rho_d\, dl\, dD_d\left(\frac{r_{\rm E}^3}{t_{\rm E}^4}\right) dt_{\rm E}\bar{f}\left(\frac{r_{\rm E}}{t_{\rm E}}\right)\ . \tag{11}$$

Since $\bar{f}(v_t)$ is independent of the geometry of the lensing tube, the integration over l is trivial:

$$d\Gamma = 2\rho_d l\, dD_d\left(\frac{r_{\rm E}^3}{t_{\rm E}^4}\right) dt_{\rm E}\bar{f}\left(\frac{r_{\rm E}}{t_{\rm E}}\right)\ . \tag{12}$$

For a PLPS, the microlensing tube section is a circle with length $l = 2u_{\rm min}\pi r_{\rm E}$, with $u_{\rm min}$ given by

$$u_{\rm min} = \sqrt{2}\sqrt{\frac{A_{\rm thr}}{\sqrt{A_{\rm thr}^2 - 1}} - 1}\ .$$

For a general lens, the tube section is much more complicated. On dimensional grounds, the length l of the lensing tube can be written as

$$l = 2\pi r_{\rm E} K(A_{\rm thr})\ . \tag{13}$$

The K-factor is a function of both the magnification threshold $A_{\rm thr}$ and the geometry of the lens (e.g., the distance of the components in Einstein units and the mass ratio of the components for a binary lens). The quantity K is not in general linear in $u_{\rm min}$. For instance, for a binary lens and $A_{\rm thr} \gg 1$, K is almost independent of $u_{\rm min}$ (see § 4.3).

Replacing l from equation (13) into equation (12) gives

$$d\Gamma = 4\pi K(A_{\rm thr})\rho_d\, dD_d \left(\frac{r_{\rm E}^4}{t_{\rm E}^4}\right) dt_{\rm E} \bar{f}\left(\frac{r_{\rm E}}{t_{\rm E}}\right) \tag{14a}$$

$$= K(A_{\rm thr})\left(\frac{d\Gamma}{dt_{\rm E}}\right)_0 dt_{\rm E}\ , \tag{14b}$$

where $(d\Gamma/dt)_0$ is the rate obtained with point sources and point lenses. Equation (14b), which was also found by Baltz & Gondolo (2001), means that the lensing rate for exotic lenses can be calculated by rescaling the lensing rate for PLPS lenses with K. The quantity K can be calculated for any observed microlensing event, provided that the geometry of the event and the magnification threshold $A_{\rm thr}$ are known. Examples of calculations are given in §§ 4.1 and 4.2.

If source stars are not resolved and differential photometry is used, the magnification threshold depends on the magnitude of the source star and has to be found on an event-by-event basis. From now on, I assume that the microlensing events are found by monitoring a catalog of resolved objects and using a fixed magnification threshold. The resolved objects are a blend of many stars. If only a fraction f of the source object flux is magnified, it is useful to define an effective magnification threshold by

$$A_{\rm thr}^{\rm eff} = \frac{A_{\rm thr} + f - 1}{f}\ . \tag{15}$$

3. ESTIMATION OF THE MICROLENSING OPTICAL DEPTH

For the purpose of calculating τ, it is convenient to calculate a weighted average of $t_{\rm E}$. One gets from equation (3) that

$$\langle t_{\rm E}\rangle = \int \frac{1}{K}\frac{d\Gamma}{dt_{\rm E}} t_{\rm E}\, dt_{\rm E} \tag{16}$$

$$= \frac{1}{N_{\rm src}T_{\rm obs}} \sum_{\rm events} \frac{p}{K(A_{\rm thr})}\frac{t_{\rm E}}{\epsilon(t_{\rm E})}\ . \tag{17}$$

Since $d\Gamma/dt_{\rm E}$ is the number of lenses entering the microlensing tube per unit time and unit $t_{\rm E}$, the observed events in the right-hand side of equation (17) have (in general) to be multiply counted. The multiplicity p is the number of observed amplification threshold crossings.

The experimental efficiency takes into account the loss of events due to selection cuts (see, e.g., Lasserre 2000) as well as time sampling. It is generally calculated with simulated microlensing light curves superposed on observed stable star light curves. It is thus clear that the experimental efficiency depends not only on $t_{\rm E}$ but also on the geometry of the lensing event and needs not be the same for binaries and PLPS lenses.

Inserting equation (14b) into the right-hand side of equation (16) gives

$$\frac{1}{N_{\rm src}T_{\rm obs}} \sum_{\rm events} \frac{p}{K(A_{\rm thr})}\frac{t_{\rm E}}{\epsilon(t_{\rm E})} = -4\pi \int \rho_d\, dD_d \int \left(\frac{r_{\rm E}^4}{t_{\rm E}^3}\right) dt_{\rm E} \bar{f}\left(\frac{r_{\rm E}}{t_{\rm E}}\right)\ . \tag{18}$$

Changing variables from $t_{\rm E}$ to $w = r_{\rm E}/t_{\rm E}$, one gets

$$\frac{1}{N_{\rm src}T_{\rm obs}} \sum_{\rm events} \frac{p}{K(A_{\rm thr})}\frac{t_{\rm E}}{\epsilon(t_{\rm E})} = 4\int \pi\rho_d r_{\rm E}^2\, dD_d \int dw\, w\bar{f}(w) \tag{19}$$

$$= 4\left[\int dw w\bar{f}(w)\right]\tau\ . \tag{20}$$

The integral over w is calculated in the Appendix. The right-hand side of equation (20) is independent of v_d, σ_x, and σ_y. Equation (20) can be rewritten as

$$\tau = \frac{\pi}{2N_{\rm src}T_{\rm obs}} \sum_{\rm events} \frac{p}{K(A_{\rm thr})}\frac{t_{\rm E}}{\epsilon(t_{\rm E})}\ . \tag{21}$$

Equation (21) is the main result of this paper and is fully discussed in § 4. For PLPS lenses, K is simply $u_{\rm min}$. For $K = u_{\rm min} = p = 1$, equation (21) gives the formula used by the microlensing surveys to derive τ from the observed Einstein radius crossing time distribution. As far as the author knows, exotic microlensing events have always been either summed up as ordinary events or just ignored. I now estimate the values of K for exotic lenses.

4. DISCUSSION

As explained in § 1, many types of exotic microlensing events have been observed. The Earth's motion in its orbit around the Sun (parallax) is detected as a small asymmetry on the light curve of microlensing events. The weight for parallax events is simply $K = 1$, because the K-factor is independent of the lensing tube drift velocity v_d. By the same argument, "xallarap" events, which are the motion of the source around a companion, also have $K = 1$.

The main effects that require a nontrivial value of K are the finite sizes of source stars and binary lenses. To give specific values, I now take as an example the events found by the MACHO collaboration (Alcock et al. 1997, 2000a) toward the LMC. Three events in the MACHO sample are possible exotic events (Dominik & Hirschfeld 1996; Alcock et al. 2000b), LMC-1 (finite size or binary lensing), LMC-9 (binary lensing), and LMC-10 (binary lensing). The asymmetric light curve of LMC-10 strongly suggests that this event can also be interpreted as a background with an eruptive variable source star. Note that LMC-9 and LMC-10 were used for estimating the microlensing optical depth toward the LMC in the 2 yr sample (Alcock et al. 1997) but were discarded in the 5.7 yr sample (Alcock et al. 2000a). The magnification threshold was $A_{\rm thr} = 1.75$ in the 2 yr sample and $A_{\rm thr} = 1.49$ in the 5.7 yr sample. Event LMC-1 can be taken as unblended. Event LMC-9 has blending coefficients in the R and B bands of $f_R \simeq 0.26$ and $f_B \simeq 0.17$ (Alcock et al. 2000b), so that its effective magnification threshold is $A_{\rm thr}^{\rm eff} \simeq 3.4$. Event LMC-10 has blending coefficients of $f_B = f_R = 0.15$, and the effective magnification threshold is $A_{\rm thr}^{\rm eff} \simeq 4.3$.

4.1. *Finite Size of Source Stars*

The magnification of extended sources depends in a complicated way on $\sigma = r_s D_s / r_{\rm E} D_d$ (Witt & Mao 1994), where r_s is the source star radius. MACHO event LMC-1 shows a deviation from the simplest PLPS microlensing model. This deviation has been modeled by various authors (Witt &

Mao 1994; Dominik & Hirschfeld 1996) as the effect of the source disk finite extent. A value of $\sigma \simeq 0.18$ has been fitted by Dominik & Hirschfeld (1996).

The microlensing light curve with extended sources has been calculated by Witt & Mao (1994). In the limit $\sigma \ll 1$, they find that the extended source light curve is a simple extension of the PLPS light curve (eq. [A4], Witt & Mao 1994):

$$A_{\rm thr}^{\rm MACHO} = \frac{2+K^2}{K\sqrt{4+K^2}} + \sigma^2 \frac{4(1+K^2)}{K^3(4+K^2)^{5/2}} . \quad (22)$$

Solving equation (22) for K and comparing with the usual impact parameter $u_{\rm min}$, which is the solution of

$$A_{\rm thr}^{\rm MACHO} = \frac{2+u_{\rm min}^2}{u_{\rm min}\sqrt{4+u_{\rm min}^2}} , \quad (23)$$

gives $K_{\rm LMC\text{-}1}^{\rm fs} = 1.008u_{\rm min}$.

The K-correction is thus within 1% of $u_{\rm min}$ in spite of the relatively large σ-value assumed here. However, as shown in § 4.3, the K-correction for a finite source effect may become important for a strongly blended source star.

4.2. *Binary Lenses*

In cases more complicated than the finite-size effect, such as binary lenses (Schneider & Weiss 1986; Mao & Paczyński 1991; Dominik 1999), the microlensing tube has a complicated shape. The total length l of the tube section has been calculated by a Monte Carlo algorithm. A small " rod " with length λ is generated in the source plane and rotated around its center. The magnification is calculated at both ends of the rod. The fifth-order equation giving the magnification of binary lenses (Witt & Mao 1995) is solved numerically. The points selected are those for which one end of the rod is above threshold and the other is under. These points cover an area $\mathscr{A}$ of width 2λ having the shape of a ribbon located along the tube slice boundary, equally spread on each side of this boundary. The length l is thus found by $l = \mathscr{A}/(2\lambda)$.

I find that the K-correction for LMC-1 is consistent with 1 at the 1% level in both MACHO binary models 1a and 1b. The K-corrections for LMC-9 and LMC-10 are

$$K_{\rm LMC\text{-}9}(1.75) = (1.49 \pm 0.04)u_{\rm min} , \quad (24a)$$

$$K_{\rm LMC\text{-}10}(1.75) = (1.11 \pm 0.03)u_{\rm min} \quad (24b)$$

for the 2 yr analysis and

$$K_{\rm LMC\text{-}9}(1.49) = (1.31 \pm 0.06)u_{\rm min} , \quad (25a)$$

$$K_{\rm LMC\text{-}10}(1.49) = (1.06 \pm 0.01)u_{\rm min} \quad (25b)$$

for the 5.7 yr analysis.

First assume that the efficiencies and blending corrections calculated with PLPS lenses can be used on binary lenses. Then the optical depth contributed by events LMC-9 and LMC-10 can be obtained by dividing the values in Table 7 of Alcock et al. (1997) and Table 8 of Alcock et al. (2000a) by the relevant K-factors. The microlensing optical depth of Alcock et al. (1997) is changed from $\tau = 2.9 \times 10^{-7}$ to 2.65×10^{-7}, an 8% effect. The optical depth of analysis B of Alcock et al. (2000a) is lowered by only 2%. In both cases, the effect is much smaller than the systematics quoted in the papers.

However, the reductions of the optical depth by 8% and 2% are only lower limits, because the blending corrections increase the detection efficiency of binaries such as LMC-9 and LMC-10 more than that of PLPS lenses. This can be seen by calculating the K-factors at the effective magnification threshold $A_{\rm thr}^{\rm eff}$ instead of the magnification threshold $A_{\rm thr}$. The K-factors are

$$K_{\rm LMC\text{-}9}(3.4) = (2.9 \pm 0.1)u_{\rm min} , \quad (26a)$$

$$K_{\rm LMC\text{-}10}(4.3) = (1.9 \pm 0.1)u_{\rm min} . \quad (26b)$$

The increase in the lensing rate of binary lenses relative to PLPS (measured by K) has to be taken into account in the blending correction of the detection efficiency.

An important question is whether lenses with distant companions (" wide binaries ") have any K-corrections, since a large (~50%) fraction of the stars are members of binary systems. The simulation shows that the K-correction for a binary star with mass ratio q and projected separation a is within 1% of 1 (assuming $A_{\rm thr} = 1.34$), as long as

$$\frac{qr_{\rm E}^2}{a^2} < 0.1 . \quad (27)$$

Assuming that the projected separation is half the space separation and using Kepler's third law, this condition can be recast as a constraint on the period P of the binary:

$$P > 452[qx(1-x)]^{3/4} \left(\frac{M_d}{M_\odot}\right)^{1/4} \left(\frac{D_s}{10\ {\rm kpc}}\right)^{3/4} {\rm yr} , \quad (28)$$

where $x = D_d/D_s$. Taking $q = 0.5$, $M_d = 0.2\ M_\odot$, and typical values $1 - x = 6 \times 10^{-2}$ ($x = 0.85$) for LMC (Galactic center) lenses, the constraint on P becomes $P > 50$ yr. The $\log P$ distribution for binaries is roughly Gaussian with an average period $P_{\rm av} \sim 6 \times 10^4$ days and $\sigma_{\log P} = 2.3$ (Duquennoy & Mayor 1991). Thus, roughly 62% of the binary lenses do not need a K-correction for an unblended source and a magnification threshold $A_{\rm thr} = 1.34$. As is seen in § 4.3, the conclusion that a large fraction of wide binaries do not need to be corrected remains valid for blended sources.

4.3. *Blending*

The examples of LMC-9 and LMC-10 show that $K/u_{\rm min}$ can be much larger than 1 for blended sources. This can be easily understood for binary lenses, since the length of the microlensing tube tends to be twice the caustics length at high $A_{\rm thr}$ (neglecting the finite size of the source) instead of 0 for PLPS lenses. For wide binaries in the high-$A_{\rm thr}$ limit, the caustic length is $\sim 8\sqrt{2}q(r_{\rm E}/a)^2 r_{\rm E}$ (Dominik 1999) so that the K-factor is

$$\frac{K}{u_{\rm min}} \simeq \frac{8\sqrt{2}}{\pi u_{\rm min}} q \left(\frac{r_{\rm E}}{a}\right)^2 \simeq 3.6qA_{\rm thr}\left(\frac{r_{\rm E}}{a}\right)^2 . \quad (29)$$

For a strongly blended source star with $A_{\rm thr}^{\rm eff} \sim 1000$, the condition $K/u_{\rm min} > 1$ gives a constraint on the period $P > 10^4$ yr. In other words, even with $A_{\rm thr}^{\rm eff} \sim 1000$, one-third (roughly) of binary lenses need not be K-corrected, but the correction for the other binary lenses, especially intermediate-type binaries such as MACHO LMC-9, may be very large.

The finite size of blended source stars can give nonnegligible values for $K/u_{\rm min} - 1$. Numerically, $K/u_{\rm min}$ is found

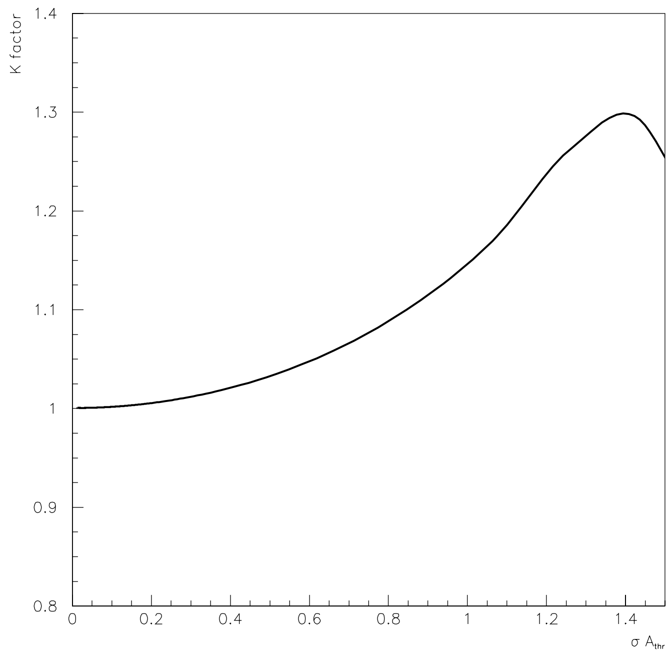

FIG. 2.—Plot of the K-factor vs. magnification threshold $A_{\rm thr}$ times σ. The quantity σ, defined in § 4.1, is the ratio of the source size to the projection of the Einstein radius of the lens onto the source plane.

to depend only on $\sigma A_{\rm thr}$, where σ is defined in § 4.1. The variation of $K/u_{\rm min}$ as a function of $\sigma A_{\rm thr}$ is shown in Figure 2. Figure 2 is very similar to Figure 3 of Schneider (1987), and the underlying physics is of course the same.

An LMC lens with $M_d = 0.1\ M_\odot$ located at 300 pc in front of the source has an Einstein radius $r_{\rm E} \simeq 0.5$ AU. The parameter σ ranges from 0.1 for a red giant source to 10^{-3} for an M dwarf. These relatively high σ-values may give nontrivial K-factors. For instance, a solar-type star inside the seeing disk of a giant star contributes only $\sim 1/100$ of the total light. The magnification threshold for such a star is thus ~ 100, and the K-factor is $\sim 1.2 u_{\rm min}$ from Figure 2.

A 0.1 $M_\odot$ lens located 1500 pc in front of the Galactic center has an Einstein radius of $r_{\rm E} \simeq 1$ AU, so that the orders of magnitude are similar to those discussed in the previous paragraph.

In microlensing surveys, the raw efficiencies and Einstein radius crossing time are generally modified to take the blending of sources into account (Alcock et al. 2001). The K-factors generally increase the efficiency for detecting blended sources and thus tend to decrease the optical depth.

5. CONCLUSION

Exotic microlensing events such as binary lensing or source finite-size effects contribute differently from the simplest point lens–point source events to the optical depth. Taking this effect into account leads to a reduction in the measured optical depth. The finite size of blended stars may give a reduction of up to 30% of the microlensing optical depth. The effect of binaries may be even larger. However, the fraction of binary microlensing events found by large statistics searches is not greater than $\sim$10% (Alcock et al. 2000b; Jaroszyński 2002). The fraction of exotic lenses may be underestimated because of the imperfect time coverage of the microlensing events (Di Stefano 2000). However, the events that give the largest correction to the optical depth are the least likely to be misidentified as ordinary lenses. Thus, it is probable that the correction to the optical depth from exotic lenses is not more than a few percent and is smaller than the 30% error on the microlensing optical depth toward the LMC (Alcock et al. 2000a) or the 15% error on the optical depth toward the Galactic bulge (Alcock et al. 2000c).

I am grateful to Andy Gould, Jacques Haissinski, and Jim Rich for many interesting comments. I also thank Clarisse Hamadache for helpful suggestions.

APPENDIX

The direction of the principal axis of the velocity dispersion tensor relative to an arbitrary (X, Y)-axis is given by the angle α. The direction of drift is given by the angle $\beta = \alpha + \delta$. One has

$$v_{({\rm dis})_x} = v_t \cos(\gamma + \Psi - \alpha) - v_d \cos\delta \ , \tag{A1}$$

$$v_{({\rm dis})_y} = v_t \sin(\gamma + \Psi - \alpha) - v_d \sin\delta \ . \tag{A2}$$

Rotating the microlensing tube is equivalent to rotating the (X, Y)-axis system or α. Hence, using equation (7), averaging over α, and keeping γ, Ψ, and δ fixed gives

$$\bar{f}(v_t) = \frac{1}{(2\pi)^2 \sigma_x \sigma_y} \int_0^{2\pi} \exp\left\{ -\frac{1}{2} \left[\frac{(v_t \cos\alpha - v_d \cos\delta)^2}{\sigma_x^2} + \frac{(v_t \sin\alpha + v_d \sin\delta)^2}{\sigma_y^2} \right] \right\} d\alpha \ , \tag{A3}$$

where $\bar{f}$ depends only on v_d and is independent of the geometry of the microlensing tube. In § 2 it was shown that τ is equal to $\sum_{\rm events}[1/K(A_{\rm thr})][t_{\rm E}/\epsilon(t_{\rm E})]$ up to a numerical factor that is the integral

$$I(\bar{f}) = \int dw\, w \bar{f}(w) \ . \tag{A4}$$

Defining w', α', δ', and v'_d as

$$w' = \sqrt{\frac{\cos^2\alpha}{\sigma_x^2} + \frac{\sin^2\alpha}{\sigma_y^2}} w \ , \tag{A5}$$

$$\tan(\alpha') = \frac{\sigma_x}{\sigma_y}\tan(\alpha) \ , \tag{A6}$$

$$\tan(\delta') = \frac{\sigma_x}{\sigma_y}\tan(\delta) \ , \tag{A7}$$

$$v'_d = \sqrt{\frac{\cos^2\delta}{\sigma_x^2} + \frac{\sin^2\delta}{\sigma_y^2}} v_d \tag{A8}$$

and changing variables from (w, α) to (w', α') gives

$$I(\bar{f}) = \frac{1}{(2\pi)^2}\int_0^\infty dw'\, w' \int_0^{2\pi} d\alpha' \ \exp\left\{-\frac{1}{2}\left[(w')^2 + (v'_d)^2 - 2w'v'_d\cos(\alpha' - \delta')\right]\right\} \ . \tag{A9}$$

Next, integrating over α' gives

$$I(\bar{f}) = \frac{1}{2\pi}\int_0^\infty dw'\, w' \exp\left\{-\frac{1}{2}\left[(w')^2 + (v'_d)^2\right]\right\} I_0(w'v'_d) \ . \tag{A10}$$

Using equation (11.4.29) of Gradshteyn & Ryzhik (1980) finally yields

$$I(\bar{f}) = \frac{1}{2\pi} \ . \tag{A11}$$

REFERENCES

Afonso, C. 2001, Ph.D. thesis, Univ. Paris
Alcock, C., et al. 1997, ApJ, 486, 697
———. 2000a, ApJ, 542, 281
———. 2000b, ApJ, 541, 270
———. 2000c, ApJ, 541, 734
———. 2001, ApJS, 136, 439
Baltz, E. A., & Gondolo, P. 2001, ApJ, 559, 41
Derue, F., et al. 2001, A&A, 373, 126
Di Stefano, R. 2000, ApJ, 541, 587
Dominik, M. 1999, A&A, 349, 108
Dominik, M., & Hirschfeld, A. C. 1996, A&A, 313, 841
Duquennoy, A., & Mayor, M. 1991, A&A, 248, 485
Evans, N. W., & Belokurov, V. 2002, ApJ, 567, L119
Gradshteyn, I. S. G., & Ryzhik, I. M. 1980, Table of Integrals, Series and Products (New York: Academic)
Griest, K. 1991, ApJ, 366, 412
Jaroszyński, M. 2002, Acta Astron., 52, 39
Lasserre, T. 2000, Ph.D. thesis, Univ. Paris
Lasserre, T., et al. 2000, A&A, 355, L39
Mao, S., & Paczyński, B. 1991, ApJ, 374, L37
Paczyński, B. 1996, ARA&A, 34, 419
Palanque-Delabrouille, N., et al. 1998, A&A, 332, 1
Popowski, P., et al. 2001, in ASP Conf. Ser. 239, Microlensing 2000: A New Era in Microlensing Astrophysics, ed. J. W. Menzies & P. D. Sackett (San Francisco: ASP), 244
Schneider, P. 1987, A&A, 179, 71
Schneider, P., & Weiss, A. 1986, A&A, 164, 237
Udalski, A., et al. 1994, Acta Astron., 44, 165
Witt, H. J., & Mao, S. 1994, ApJ, 430, 505
———. 1995, ApJ, 447, L105